

Laser Propulsion Using Free Electron Lasers

Dennis Keefer,* Ahad Sedghinasab,† Newton Wright,‡ and Quan Zhang§
University of Tennessee Space Institute, Tullahoma, Tennessee 37388

Quasisteady plasmas have been initiated and sustained in argon at pressures from one to three atmospheres using power absorbed from a 10.6- μm wavelength laser beam produced by the RF linac free electron laser at Los Alamos National Laboratory. The pulse format of the RF linac laser consisted of an 80- μs -long burst of 10 ps pulses separated by 46 ns, with an average power of approximately 3.75 kW. Time-resolved spectroscopic observations revealed no decay of the plasma during the 46 ns interpulse time. Analysis of the spectroscopic data using Boltzmann factors, ion-neutral intensity ratios, and absolute emission coefficients gave values of the plasma temperature that varied from 17,500 K to 20,000 K during the 80- μs pulse. Attempts to obtain optical breakdown in nitrogen and hydrogen proved unsuccessful, even at optical intensities ten times the observed threshold for argon.

I. Introduction

IN a propulsion system supported by a laser-sustained plasma (LSP), the high-power laser beam from a remote site is focused into the thruster. The plasma is ignited and continuously sustained near the laser focus. The plasma is used to absorb the power from the laser beam and convert it into propellant enthalpy.

Application of high-power laser sustained plasmas (LSP) to space propulsion technology requires a fundamental understanding of the mechanisms by which a laser beam can initiate and sustain a plasma under various flow and power conditions. Interactions between the laser beam and the flowing plasma is complex and highly nonlinear, and detailed experiments have been required to gain a quantitative understanding of these processes.¹ A series of experimental investigations has been conducted at The University of Tennessee Space Institute (UTSI) using a 1.5 kW continuous (CW) CO₂ laser to obtain detailed measurement of the plasma temperature field in an argon LSP.² Laser power absorption and radiative emission were calculated from the measured temperature field to provide a detailed understanding of the energy conversion processes. Based upon the experimental results, a detailed computational model was developed that provides a comprehensive description of the LSP in convective flow environments.³ Similar work has been performed at The University of Illinois using a CW CO₂ laser at powers up to 10 kW and with a maximum flow velocity of 30 m/s at a pressure of one atmosphere.⁴ Plasma absorption and thermal efficiencies using various gas mixtures and optical configurations were the main focus of these experiments. The computational code developed at UTSI was extended to provide a detailed design for a 30 kW laser powered thruster using hydrogen as a propellant.⁵

A comprehensive evaluation of laser-based propulsion systems has determined that lasers in the megawatt power range will be required to ensure the practicality of this concept.⁶ Presently, pulsed free electron lasers (FEL) seem to be the

most promising way to provide these power levels. These lasers can provide both nanosecond and picosecond pulses, but the RF Linac laser may be able to provide a quasicontinuous beam consisting of trains of picosecond pulses. Optical plasma breakdown using pulsed CO₂ lasers has been studied for two decades, but these experiments were all conducted using essentially single laser pulses of nanosecond or longer duration. We conducted these experiments at Los Alamos National Laboratory (LANL) to evaluate the feasibility of using the RF Linac laser to sustain quasisteady plasmas.

Prior to the experiments performed at LANL, the decay characteristics of argon optical breakdown plasmas were studied at the Center for Laser Applications at The University of Tennessee Space Institute using a Lumonics XeCl excimer laser with wavelength of 308 nm and pulsewidth of approximately 20 ns. An optical multichannel analyzer (OMA) was used to record the radiation spectrum of the argon plasma created within a closed cell. Spectra were recorded in 10-ns steps with 10-ns gatewidth for up to 15 μs after the plasma initiation. These preliminary studies indicated that the decay rate of an argon optical breakdown plasma is of the order of microseconds, which is much longer than the interpulse time of the LANL laser, and suggested that it was feasible to sustain an argon plasma with the pulse format of the LANL RF Linac free electron laser.

In the following sections we describe the experimental facilities, experimental procedures, spectral data reduction, and plasma temperature determination using several spectroscopic techniques.

II. Experiment

A quasisteady argon plasma was sustained by the LANL free electron laser in a flow chamber that was constructed with zinc selenide windows on both ends so that a direct measurement of laser absorption could be obtained. The flow tube, where the plasma was sustained, had a diameter of 1 cm to provide relatively high incident flow velocities at moderate mass flow rates. An annular flow was provided at the surface of the entrance window to provide cooling.

The RF linac free electron laser was tuned to a wavelength of 10.6 μm to provide direct comparison with the experiments performed using CO₂ lasers. The output beam of the FEL operated in a gaussian TEM₀₀ mode with 80–120- μs macropulses, which were repeated at a rate of 1 Hz. The macropulse energy was approximately 300 mJ, giving an average power of 3.75 kW during an 80- μs burst. Each 80- μs burst consists of approximately 1700 micropulses that have a duration of approximately 10 ps and are spaced 46 ns apart to provide a peak power of about 17 MW. The laser output beam was

Presented as Paper 90-2636 at the AIAA/DGLR/JSASS 21st International Electric Propulsion Conference, Orlando, FL, July 18–20, 1990; received Dec. 10, 1990; revision received Aug. 20, 1991; accepted for publication Sept. 25, 1991. Copyright © 1990 by the American Institute of Aeronautics and Astronautics, Inc. All rights reserved.

*Professor of Engineering Science and Mechanics, Center for Laser Applications. Member AIAA.

†Research Associate, Center for Laser Applications.

‡Engineer, Center for Laser Applications.

§Graduate Research Assistant, Center for Laser Applications.

focused into the flow chamber by a zinc selenide lens with focal length of 127 mm. The spot size was calculated to be about $95 \mu\text{m}$ in diameter resulting in a peak power density of 10^{11} W/cm^2 for a 120-mJ macropulse.

A variety of diagnostic measurements were made during the experiment. A Hadland image converter camera was interfaced with a CID video camera to provide digital images, which were acquired using a Matrox framegrabber housed in a Masscomp computer. This provided high-speed images of the transient plasma formation and decay at a framing rate of 100,000 frames per second. Time resolved spectra of the plasma were obtained using the OMA in a manner similar to that used for the excimer laser generated plasma. The OMA gatewidth was set to 10 ns, and 10 spectra were accumulated from 10 successive macropulse breakdowns to average the results of several realizations of the plasma and to enhance the signal-to-noise ratio. The OMA was then delayed for 10, 20, 30, 40, and 50 ns, and the spectral data accumulation was repeated for each delay setting. Similar spectra were also obtained at 20- μs intervals throughout a 120- μs burst. The OMA was calibrated for absolute intensity using both tungsten ribbon and deuterium arc standard lamps. Wavelength calibration was obtained using mercury and argon spectral sources. A schematic of the experimental apparatus is shown in Fig. 1.

Data were obtained for FEL sustained argon plasmas at pressures of 1 and 3 atm over a range of incident flow velocities. These plasmas were easily initiated at all pressures, and nearly complete absorption of the incident laser beam was measured by the two energy meters installed upstream and downstream of the flow chamber.

Hydrogen and nitrogen gases were also introduced to the flow chamber, in separate experiments, in an attempt to study the differences in the initiation and plasma characteristics between these gases and argon. However, self-initiation was never achieved in these molecular gases, even at ten times the power required for argon breakdown.

III. Spectral Data Reduction

The spectral data acquired by the OMA were calibrated for both wavelength and absolute intensity. Spatially calibrated framing camera images were used to determine the plasma shape and size. The contribution of the continuum radiation to the absolute values of the spectral lines of interest was subtracted by fitting a straight line to the adjacent continua of that line. To determine the absolute intensity of the overlapping lines Lorentzian profiles were fitted to the lines, because Stark broadening is the dominant broadening mech-

anism for atmospheric pressure argon plasmas. The plasma was assumed to be optically thin, because the measured absolute emission coefficients described below yielded an optical thickness of about 6×10^{-3} .

Several different spectroscopic methods were used to calculate the argon plasma temperature from the plasma intensity measurements. The first method used the relative emission coefficient ratio of an argon ion line and a neutral line given by⁷

$$\frac{I_i}{I_a} = 2 \frac{\lambda_a A_i g_i}{\lambda_i A_a g_a} \left(\frac{2\pi m_e kT}{h^2} \right)^{3/2} \frac{1}{n_e} \exp\left(-\frac{E_i - E_a}{kT} \right)$$

where

$$I = \int_{\Delta\lambda} I(\lambda) d\lambda \quad (1)$$

The subscripts i and a refer to ion and neutral. λ is the transition wavelength, $\Delta\lambda$ is the total width of the line at the continuum base, A is the transition probability, g is the statistical weight of the transition upper level, n_e is the electron density, E is the upper level energy relative to the ground state of the neutral atom, and k is the Boltzmann constant. This method requires a knowledge of the electron density. The electron density can be obtained by an iterative solution of the ideal gas law and the Saha equations at the measured pressure, with the assumption of two stages of ionization, quasineutrality, and local thermodynamic equilibrium (LTE):

$$p = (n_e + n_i + n_{ii} + n_a)kT \quad (2)$$

$$n_e = n_i + 2n_{ii} \quad (3)$$

$$\frac{n_e n_i}{n_a} = \frac{2Z_i}{Z_a} \left(\frac{2\pi m_e kT}{h^2} \right)^{3/2} \exp\left(-\frac{E_i}{kT} \right) \quad (4)$$

$$\frac{n_e n_{ii}}{n_i} = \frac{2Z_{ii}}{Z_i} \left(\frac{2\pi m_e kT}{h^2} \right)^{3/2} \exp\left(-\frac{E_{ii}}{kT} \right) \quad (5)$$

Here subscript ii denotes the second stage of ionization, Z is the electronic partition function, E_i is the first ionization potential, E_{ii} is the second ionization potential, and p denotes the chamber pressure.

The uncertainty in the resulting values of temperature based on the uncertainties of other parameters in Eq. (1) can be estimated as

$$\frac{\Delta T}{T} \approx \left[\frac{\Delta(I_i/I_a)}{I_i/I_a} + \frac{\Delta(A_i/A_a)}{A_i/A_a} + \frac{\Delta n}{n_e} \right] \frac{kT}{E_i - E_a} \quad (6)$$

For $T = 20,000 \text{ K}$, $(E_i - E_a)/kT \approx 14$ for the spectral lines considered here. Therefore, even significant uncertainties in I_i/I_a or n_e , would only result in a small error in the temperature values.

In the second method, the relative upper level populations of argon ion lines are obtained from the relative intensity of the lines using

$$n_m = C \frac{\lambda_{mn}}{A_{mn}} I \quad (7)$$

where C is the proportionality constant. The logarithm of level population ratios are then plotted against the upper level energies. Boltzmann factors given by

$$\log\left(\frac{n_m/g_m}{n_n/g_n} \right) = -\frac{1}{T} \left(\frac{E_m - E_n}{k} \right) \quad (8)$$

are then used to determine the plasma temperature from the slope of a straight line, which is least-squares-fitted to all the

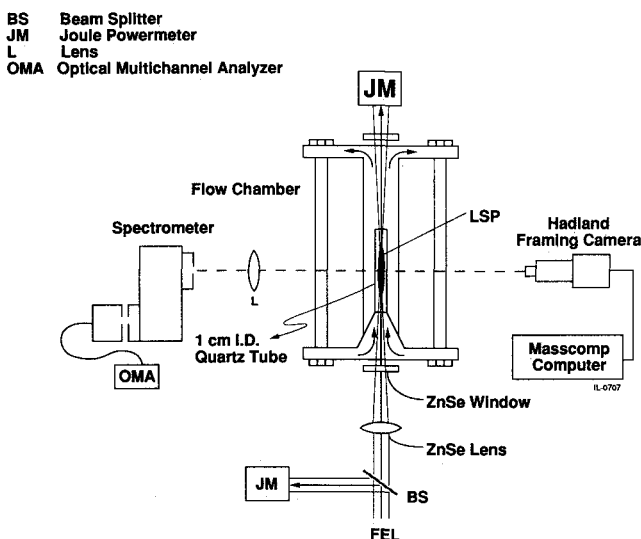


Fig. 1 Schematic of the experimental diagnostic configuration.

points on the plot. This method assumes that the upper level densities of all the measured lines are distributed according to a single equilibrium temperature. The accuracy of this method depends both upon the number of spectral lines used and differences in their energy levels.

In the third method, the temperature was calculated from the line emission coefficient, which was determined from the measured absolute line intensity I_{abs} using

$$\varepsilon_L = \frac{I_{\text{abs}}}{\ell} \quad (9)$$

where ℓ is the length of the plasma in the direction of line of sight. The value of ℓ was obtained from the framing camera images. The upper level populations of the ionic lines are then calculated from

$$n_m = \frac{4\pi\lambda_{mn}\varepsilon_L}{hcA_{mn}} \quad (10)$$

The ionic ground state density is related to the upper level densities by the Boltzmann factor

$$\frac{n_m}{n_i} = \frac{g_m}{Z_i} \exp\left(-\frac{E_m}{kT}\right) \quad (11)$$

If we assume that the plasma is in LTE, then Eqs. (2–5) and Eq. 11 can be solved simultaneously to yield plasma temperature and composition.

In each of the methods described above, spatially averaged intensity data were used to calculate the plasma temperature. Because the relative intensities were used in the first two methods, the error introduced by intensity averaging is minimal. However, in the third method, where absolute intensities were used, the use of spatially averaged intensities may introduce a more significant source of error. On the other hand, the intensity and temperature profiles of LSPs are relatively flat over most of the plasma, except for a small region near the boundaries, and the temperatures calculated using this technique are expected to be reasonable representations for the central portion of the plasma.

IV. Results

Quasisteady argon plasmas were routinely self-initiated and sustained using the LANL free electron laser pulse format. Figure 2 shows the argon spectra taken each 10 ns for a total of 60 ns to ensure the inclusion of at least one micropulse.

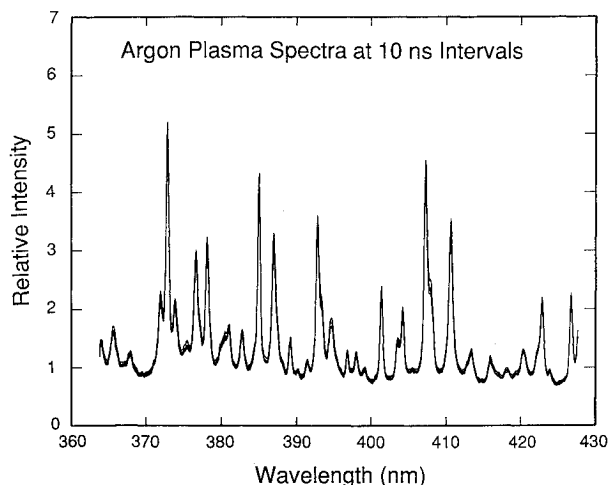


Fig. 2 Argon plasma spectra obtained using 10-ns exposures. Six spectra were obtained at 10-ns intervals to include at least one micropulse, and all six spectra are superimposed in the plot.

This figure shows no significant difference between the spectrum that included the 10-ps pulse and those spectra taken during the 46-ns interpulse time. This result probably reflects the fact that the micropulse from the laser is “on” only 1/1000 of the total 10-ns gate time of the OMA. Because of this low duty cycle, any unique spectral feature characteristic of the micropulse absorption would have little contrast relative to the background spectrum. In fact, the background spectrum exhibits no measurable change over the 46-ns interpulse time, indicating that the relaxation processes of the plasma are considerably longer than the interpulse time. This is to be expected, because most of the spectral lines in the recorded spectral range have transition times of the order of 100 ns. The only lines in ionic argon that have transition times of a few nanoseconds are the resonance lines, which were not recorded during these experiments. The argon plasma spectra recorded at 20- μ s intervals during one macropulse is shown in Fig. 3. The lowest line in this figure corresponds to the signal taken at 100 μ s, at which time, the plasma has expanded and decayed more noticeably.

Plasma temperatures calculated using the ion-neutral line ratio method are presented in Fig. 4. In this method, the relative emission coefficients of ion lines 3729, 3765, 3780, 3850, 3868, 3928, 4013, 4072, and 4103 \AA were compared to those of argon neutral lines 4158 \AA and 4200 \AA . The plasma

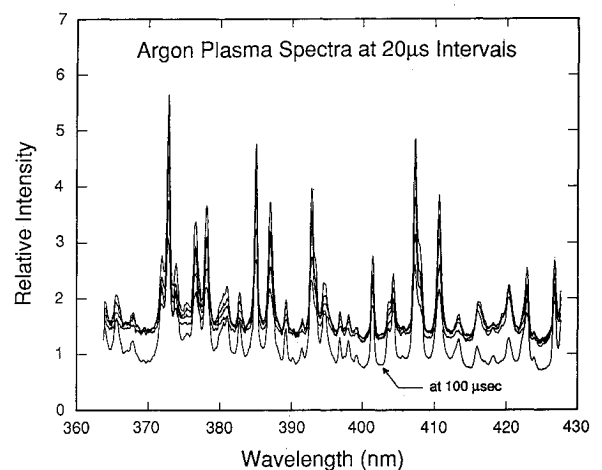


Fig. 3 Argon plasma spectra obtained using 10-ns exposures. Five spectra were obtained at 20- μ s intervals, and all five spectra are superimposed in the plot.

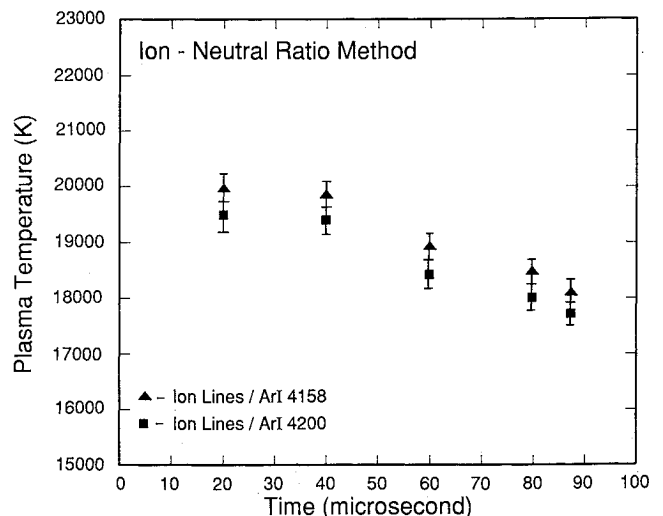


Fig. 4 Plasma temperatures obtained using the ion to neutral line ratio.

temperature is plotted vs time during one macropulse. The bars on each data point indicate the standard deviation of the temperature as determined from each of the 18 ion-neutral line pairs evaluated for the six sets of spectral data recorded at the 10-ns intervals. This scatter can be attributed to the errors involved in the deconvolution of the overlapping spectral lines, the assumption of plasma homogeneity, and the more basic uncertainties of the transition probability values.

Figure 5 shows a typical Boltzmann plot where the relative populations of various ionic excited levels are plotted vs the excited level energies. The slope of the fitted straight line is inversely proportional to the plasma temperature. The scatter in Fig. 5 is primarily associated with the process of deconvolving the overlapping lines using fitted Lorentz profiles and straight line subtraction of the continuum. Transition probability uncertainties do not play an important role in the extent of the scatter in this case, because the relative values of the transition probabilities are usually accurate to within 5% for a single ionic species.⁸ Plasma temperatures obtained by this method are shown in Fig. 6.

In the last technique where the temperature has been determined from absolute line emission, the characteristic dimension of the plasma along the line-of-sight was obtained from the framing camera images, one of which is shown in Fig. 7. The calculated plasma temperature (Fig. 8) using this technique is fairly insensitive to the value used for the plasma size. A 50% error in the plasma diameter results in only a

4% change in the value of the calculated temperature for this particular temperature range. The bars on the temperature values represent one standard deviation resulting from the use of nine different ion lines. As noted in Figs. 4, 6, and 8, the plasma temperature decreased with time, due to the expansion of the plasma about the focal region.

Although argon plasmas were easily self-initiated and sustained using the LANL free electron laser, we were unable to obtain optical breakdown in either nitrogen or hydrogen. In a laser sustained plasma at a wavelength of $10.6 \mu\text{m}$, the dominant process of laser absorption is inverse bremsstrahlung, in which the electrons are accelerated in the strong electric field (10^9 V/m in this case) created by the laser, and subsequently undergo elastic, inelastic, and ionizing collisions with neutral atoms. However, prior to breakdown there are few electrons available in the cold gas, and the electron neutral collision frequency is approximately 1 per picosecond. Therefore, it is likely that breakdown does not occur within the first micropulse, but cascades to breakdown after several micropulses. Because the rate of optical energy absorption and the ionization potential are similar for the various gases used in our experiments, it is likely that the electron loss processes that take place during the 46 ns interpulse time is responsible for the observed differences in breakdown threshold. These loss processes include excitation of internal energy states of the molecular species, electron diffusion and, in the later phases of the breakdown cascade, gasdynamic expansion. Each of these processes proceed at considerably different rates for argon and the molecular gases, and are likely to

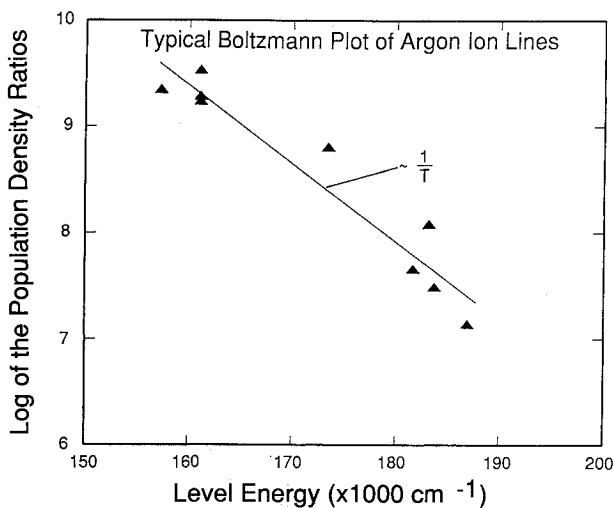


Fig. 5 Typical Boltzmann plot for the argon ion lines.

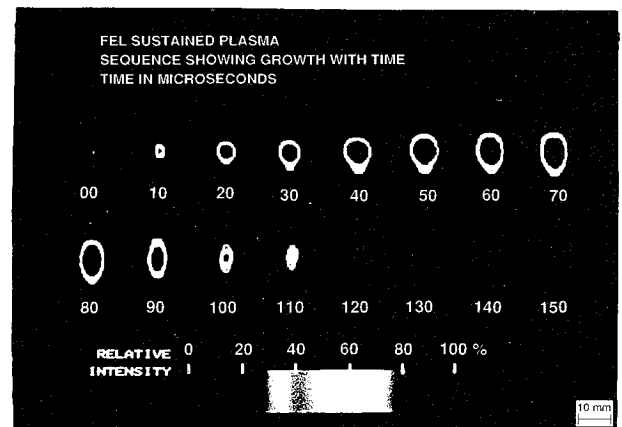


Fig. 7 Images of the plasma formation and decay obtained at 100,000 frames per second. The laser direction is from bottom to top.

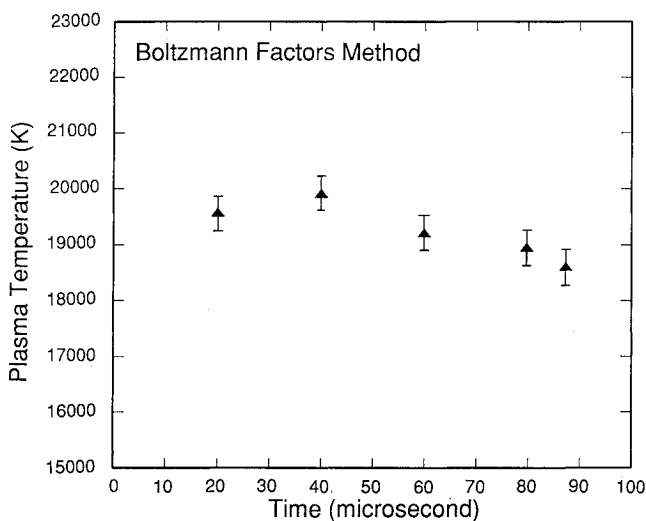


Fig. 6 Plasma temperatures obtained using the Boltzmann factors.

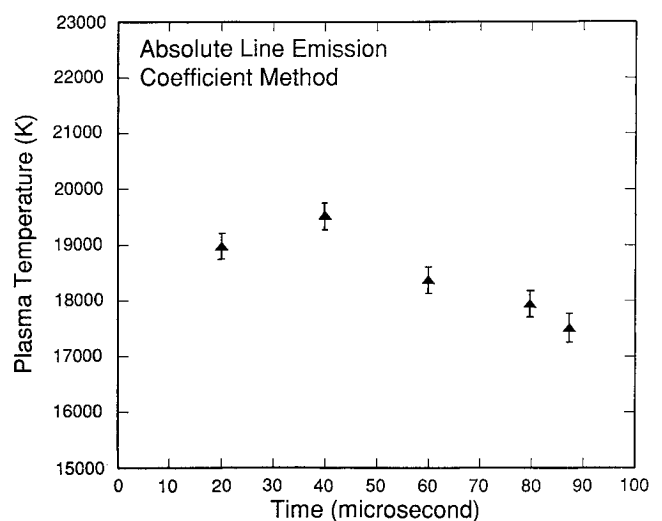


Fig. 8 Plasma temperatures obtained using absolute line emission.

be responsible for our failure to observe optical breakdown in hydrogen and nitrogen.

A detailed comparison of various features of FEL sustained plasmas to those of CO₂ laser sustained plasmas is not possible at this time due to the preliminary nature of the experiment. In this work, parameters such as flow rate, optical depth of field, and pressure were not studied to their full extent. However, it is possible to conclude that argon plasmas were sustained by FEL, which has a vastly different pulse format. The absorption of the laser energy by the plasma as measured by the Joule power meters were comparable to those encountered in CW CO₂ experiments (80–90%).

V. Conclusions

The principal conclusions that can be drawn from these initial experiments are as follows:

1) Argon plasmas are easily self-initiated and sustained by the LANL free electron laser operating at 10.6 micrometers with 10-ps micropulses.

2) Spectral data taken with 10-ns gate times at 10-ns intervals did not reveal any changes in plasma radiation during the 46-ns interpulse time.

3) The various spectroscopic techniques used to calculate the plasma temperatures yielded temperature of 17,500 K–20,000 K, depending upon the time during a macropulse.

4) Argon plasmas self-ignited at a power density of 10¹¹ W/cm², but hydrogen and nitrogen did not undergo optical breakdown for power densities up to 10¹² W/cm².

This experiment demonstrated the feasibility of using pulsed free electron lasers to ignite and sustain plasmas in a forced convection environment that could be used for space propulsion. Further experimental and theoretical research should be focused on the mechanisms responsible for the observed differences between picosecond optical breakdown thresholds in argon and the molecular gases.

Acknowledgments

This work was supported by the Air Force Office of Scientific Research under Grant AFOSR-86-0317. The authors thank Larry Warner, Jon Sollid, Dodge Warren, and the entire crew at the FEL facility at Los Alamos National Laboratory for their expert and enthusiastic support during our experiments there.

References

- ¹Keefe, D. R., "Laser Sustained Plasmas," *Laser Induced Plasmas and Applications*, edited by L. J. Radziemski and D. A. Cremers, Marcel Dekker, New York, 1989, Chap. 4, pp. 169–206.
- ²Welle, R., Keefe, D., and Peters, C., "Power Absorption in Laser-Sustained Argon Plasmas, Part I," *AIAA Journal*, Vol. 24, No. 10, 1986, p. 1663.
- ³Jeng, S. M., Keefe, D. R., Welle, R., and Peters, C. E., "Laser-Sustained Plasmas in Forced Convective Argon Flow, Part II: Comparison of Numerical Method with Experiment," *AIAA Journal*, Vol. 25, No. 9, 1987, pp. 1224–1230.
- ⁴Krier, H., Mazumder, J., Zerkle, D. K., Schwartz, S., and Meretogul, A., "Laser Sustained Argon Plasma for Thermal Rocket Propulsion," *Journal of Propulsion and Power*, Vol. 6, No. 1, 1990, pp. 38–45.
- ⁵Jeng, S. M., and Keefe, D., "Theoretical Evaluation of Laser-Sustained Plasma Thruster Performance," *AIAA Journal*, Vol. 5, No. 5, 1989, pp. 577–581.
- ⁶Kantrowitz, A., "Laser Propulsion to Earth Orbit—Has Its Time Come?" In "Visions of Tomorrow; A Focus on National Space Transportation issues," *Proceedings of the Twenty-fifth Goddard Memorial Symposium*, Greenbelt, MD, March 18–20, 1987.
- ⁷Venugopalan, M., "Reactions Under Plasma Conditions," Vol. 1, Wiley Interscience, New York, 1971, p. 396.
- ⁸Sedghinasab, A., "Experimental Determination of Argon Atomic Transition Probabilities Using Non-LTE Diagnostics," Ph.D. Dissertation, Georgia Inst. of Technology, Atlanta, GA, Dec. 1987.